Influence of spatiotemporally correlated noise on structure formation in excitable media

H. Busch* and F. Kaiser

Institute of Applied Physics, Darmstadt University of Technology, 64289 Darmstadt, Germany
(Received 29 October 2002; published 25 April 2003)

We discuss the influence of additive, spatiotemporally correlated (i.e., colored) noise on pattern formation in a two-dimensional network of excitable systems. The signature of spatiotemporal stochastic resonance (STSR) is analyzed using cross-correlation and information theoretic measures. It is found that the STSR behavior is affected by both the spatial and temporal correlations of the noise due to an interplay with the length scales of the deterministic network. Increasing the spatiotemporal noise correlation shifts the occurrence of STSR to smaller values of the noise variance. Additionally, if the spatial correlation of the noise exceeds that of the network, the excitation patterns disappear in favor of cloudy structures, directly rendering the underlying spatial noise field.

I. INTRODUCTION

Spatiotemporal pattern formation has been in the focus of interest for a long time already. Often these patterns emerge abruptly, when a critical value of a (slowly drifting) control parameter is passed (see, e.g., Refs. [1,2]). Noise-induced spatiotemporal pattern formation, also known as spatiotemporal stochastic resonance (STSR), was first investigated by Jung and Mayer-Kress in an excitable cellular-automata-like system [3]. STSR is a phenomenon, wherein spatial excitation patterns, such as target or spiral waves, are induced by fluctuations acting upon the system, showing an optimal coherence at some intermediate noise intensity. In recent years, there have been investigations verifying the existence of such an effect in two- [4–7] and three-dimensional [8,9] models, including chemical [5,6,10] and biological [11] systems. Except for Ref. [7], all of the above mentioned phenomena are reported to occur in subexcitable media, i.e., waves traveling through the system are not supported without any external (deterministic or stochastic) driving.

In most models of biological systems, fluctuations are included using white noise. The term ''white'' refers to the fact that the noise amplitudes are uncorrelated in both space and time. However, for many systems spatiotemporally correlated, i.e., colored, noise yields a more appropriate approximation of the actual fluctuations present. Temporally colored noise may provide a more accurate description, if there is an incomplete separation of stochastic and deterministic time scales [12]. Spatially colored noise may be relevant for biological systems, if they are exposed to a combination of both internal and external fluctuations with the former acting locally and the latter acting nonlocally over the whole system [13,14]. Recently, interesting effects in subexcitable media such as lifetime prolongation of spatial structures in Ref. [8] and wave train propagation [15] have been discussed, all of which are shown to be optimal at an intermediate range of spatiotemporal noise color. Due to its importance for the modeling of biological systems, it is interesting to study the

dependence of STSR on noise color, e.g., to test for the robustness of the phenomenon.

Currently, there exist no standard set of observables for extracting the signature of STSR in extended media, which has led to a huge amount of quantification attempts, in many cases applicable for a single model or experiment, only. Frequent analysis tools have been driving the system with a solitary wave [3], characterizing the spatiotemporal dynamics through the propagation distance of waves entering the noisy subexcitable medium [6,10] or cluster-size analysis of active sites in space and/or time [7,16]. For example it is observed in experiments of the photosensitive Belousov-Zhabotinsky reaction [5] and in tissues of glial cells [11], that optimal noise-induced pattern formation is associated with a power-law distribution of the cluster sizes of active sites.

Recently, Goychuk and Hänggi [17] have proposed a unifying quantification of temporal stochastic resonance (SR) using information theoretic measures that identify the effect of SR with an increased rate of information gain. In analogy to Goychuk and Hänggi, we identify STSR with an increase of *spatial* information gain. Therefore we use analysis tools, which are capable of interpreting the data in terms of local nearest-neighbor interactions. For this we employ two complementary analysis methods, a linear cross-correlation measure and the mutual information [18], the latter being capable of measuring nonlinear dependencies as well. In Ref. [19] a method similar to the cross correlation used in this paper, has been proposed and tested to find STSR in spatiotemporal data sets when the noise intensity is not known experimentally.

Following this line of thought, the structure of our paper is as follows: first we introduce the model system, and the noise generation algorithm (Sec. II). We briefly describe the tools for analyzing the data, and then we apply them to time series consisting only of noise as a first test (Sec. III). Next, we systematically investigate the influence of spatial and temporal noise color and strength on the formation of coherent spatial structures in our model system (Sec. IV). The systematics of these results are discussed in Sec. V.

II. THE MODEL

The system under consideration is a FitzHugh-Nagumo-like excitable medium, first proposed by Barkley *et al.* [20],

---

*Electronic address: Hauke.Busch@physik.tu-darmstadt.de

having piecewise linear nullclines. The equations read

$$\frac{\partial u}{\partial t} = \frac{1}{\epsilon} f(u,v) + D_c \nabla^2 u; \quad \frac{\partial v}{\partial t} = g(u,v). \tag{1}$$

The dynamical variables u and v denote the fast activator and slow inhibitor dynamics, respectively, their time scales being separated through the small, positive parameter ϵ. The model has been extensively investigated in the literature. By choice of suitable deterministic functions for $f(u,v)$ and $g(u,v)$, Eqs. (1) show typical excitation patterns such as spiral and scroll waves in two and three dimensions [20,21], respectively, and even spiral turbulence [22]. Under the influence of suitable parametric noise, the system exhibits spiral chaos [7] and STSR [23]. Due to its rich dynamical features, the Barkley system [Eq. (1)] has been used to model neuronal excitation [24], CO diffusion on a catalytic surface [25], and noise-induced waves in a photosensitive Belousov-Zhabotinsky reaction [5].

Here, we choose $f(u,v)$ and $g(u,v)$ as

$$f(u,v) = u(1-u)(u-u_{thr}), \tag{2}$$

$$g(u,v) = u - v + \xi(\mathbf{r},t); \quad u_{thr} = a(v+b). \tag{3}$$

The local dynamics in the absence of noise are governed by a stable fixed point at the origin with the function u_{thr} determining the bifurcation point and thus the system's excitability.

The diffusion term in Eq. (1) is numerically integrated on a square $N \times N$ grid with free boundary conditions. We employ nearest-neighbor coupling for evaluating the Laplacian operator

$$\nabla^2 u_{ij} = \frac{1}{6\Delta h^2} (u_{i-1,j-1} + u_{i-1,j+1} + u_{i+1,j-1} + u_{i+1,j+1}$$

$$+ 4u_{i-1,j} + 4u_{i+1,j} + 4u_{i,j-1} + 4u_{i,j+1} - 20u_{i,j}), \tag{4}$$

where we used a spatial discretization $\mathbf{r} = (x,y) = \Delta h(i,j)$ of the continuous variable $\mathbf{r}$ with a spatial gridding of $\Delta h = 0.5 s.u.$ (space units) and the indices i,j running from $i,j = 1 \cdots N = 128$.

The role of the additive noise term $\xi(\mathbf{r},t)$ is to modulate the system's excitability threshold u_{thr} via the inhibitor variable v. The spatiotemporally correlated noise field $\xi(\mathbf{r},t)$ is generated by convolving spatially incoherent, temporally correlated Gaussian noise $\zeta(\mathbf{r},t)$ with a correlation function $C(\mathbf{r})$ that is periodic in space and radially symmetric around the origin. For the sake of free boundary conditions for the Barkley system, we choose a period of $L = 2Nh$ for $C(\mathbf{r})$. In the case of spatial discretization the noise algorithm reads

$$\xi_{ij}(t) = \left(\frac{1}{2N}\right)^2 \sum_{n,m=1}^{2N} \zeta_{ij}(t) C_{n-i,m-j}, \tag{5}$$

where $\zeta_{ij}(t)$ is temporally correlated noise generated through an Ornstein-Uhlenbeck process

$$\dot{\zeta}_{ij}(t) = -\frac{1}{\tau} [\zeta_{ij}(t) + \eta_{ij}(t)], \tag{6}$$

τ denotes the temporal correlation and η_{ij} is Gaussian noise of the intensity σ^2, δ correlated both in space and time,

$$\langle \eta_{ij}(t) \eta_{i'j'}(t') \rangle = \sigma^2 \delta_{ii'} \delta_{jj'} \delta(t-t'). \tag{7}$$

The discrete correlation function C_{ij} is given by

$$C_{ij} = \frac{2}{\pi \lambda^2} \exp - \left(\frac{2\Delta h^2(i^2+j^2)}{\lambda^2} \right), \tag{8}$$

with λ controlling the spatial decay of C_{ij} and thus determining the spatial correlation of the noise field.

Summarizing, the above algorithm yields colored noise with zero mean and the following spatiotemporal correlation,

$$\langle \xi_{ij}(t) \xi_{i'j'}(t') \rangle = D \exp - \left(\frac{\Delta h^2[(i-i')^2+(j-j')^2]}{\lambda^2} \right.$$

$$\left. + \frac{|t-t'|}{\tau} \right), \tag{9}$$

where $D = \sigma^2/\tau$ corresponds to the variance of the noise, which we will refer to as noise strength in the following, and σ^2 denoting the noise intensity. Consequently, the noise field ξ_{ij} is exponentially correlated in time and Gaussian correlated in space with decay constants τ and λ, respectively.

Fourier transforming Eq. (9) yields at the continuum limit the power spectral density (P) in the temporal (ω) and spatial ($\mathbf{k}$) frequency domain

$$P(\omega,k) = D \frac{2\sqrt{\pi}\tau\lambda}{1+(\tau\omega)^2} e^{-\lambda^2 \mathbf{k}^2/4}. \tag{10}$$

Equation (5) is simulated through multiplication of C_{ij} and ζ_{ij} in Fourier space. For the particular choice for C_{ij}, being a Gauss function, symmetric in space, its Fourier transform remains real, thus reducing the number of multiplications in the complex Fourier space. Furthermore, to make the algorithm computationally more efficient, we iterated Eq. (6) directly in Fourier space [26].

Starting from random initial conditions, Eq. (1) has been numerically integrated using an implicit integration scheme and an explicit Euler method with $\Delta t = 0.007 t.u.$ (time units) for the u and v variable, respectively [21]. Throughout this paper we use the following set of parameters $(\epsilon,a,b,D_c) = (0.05, 1.18, 0.076, 1)$. They are adjusted to yield the network in a subexcitable state, i.e., the formation and preservation of spatial patterns is only possible in the presence of noise.

III. ANALYSIS TOOLS

In this paper we try to discern the noise's parameter ranges, in which the Barkley system exhibits the most coherent spatial pattern. The formation of those structures is opti-

mal, if stochastic forcing and local interactions make nearest neighbors oscillate at some fixed phase difference. Hence, it seems natural to employ tools that are efficient in analyzing nearest-neighbor relationships in space and time, namely, a linear spatial cross-correlation measure S and the pointwise mutual information I.

We compute the cross correlation S for the v variable as the space and time averaged nearest-neighbor distance of all elements, normalized by the total spatial amplitude variance.

Defining the spatial variance at time t as

$$\text{Var}(t) = \frac{1}{N^2} \sum_{ij} (v_{ij} - \bar{v})^2, \qquad (11)$$

where $\bar{v} = N^{-2} \Sigma_{ij} v_{ij}$, and defining the purely spatial autocovariance of nearest neighbors as

$$\text{Cov}(t) = \frac{1}{N^2} \sum_{ij} \frac{1}{|\mathcal{N}_{ij}|} \sum_{b \in \mathcal{N}_{ij}} (v_{ij} - \bar{v})(b - \bar{v}), \qquad (12)$$

with b consisting of all $|\mathcal{N}_{ij}| = 4$ elements of a von Neumann neighborhood $\mathcal{N}_{ij}$ at each lattice site v_{ij}, S is given by

$$S = \left\langle \frac{\text{Cov}(t)}{\text{Var}(t)} \right\rangle_T, \qquad (13)$$

where the brackets $\langle \rangle_T$ denote averaging over the total integration time T. If the network is completely synchronized in space and time, S takes up a maximal value of one. The choice of the neighborhood type was mainly done for computational ease. Using different neighborhoods for b did not change the results qualitatively.

The mutual information I is calculated by mapping the continuous variables v_{ij} on a binary state space $\Sigma \in \{0,1\}$ using a fixed threshold value v_{th},

$$\tilde{v}_{ij} = \begin{cases} 1, & v_{ij} \geqslant v_{\text{th}} \\ 0, & v_{ij} < v_{\text{th}}. \end{cases} \qquad (14)$$

This leads to the following expression for I,

$$I = \left\langle \sum_{kl \in \Sigma} p_{kl}^{ijb} \ln\left(\frac{p_{kl}^{ijb}}{p_k^{ij} p_l^b} \right) \right\rangle_{\mathcal{N}_{ij}}, \qquad (15)$$

where the brackets $\langle \rangle_{\mathcal{N}_{ij}}$ stand for averaging over the (von Neumann) neighbors b of all network elements. p_k^{ij}, p_l^b denote the state space densities of some network element $\tilde{v}_{ij}$ and its respective neighbors, with p_{kl}^{ijb} denoting their joint probability.

The mutual information yields the symmetric amount of deterministic dependence of two processes. I vanishes, if the processes are stochastically independent and obtains some positive value in case of even nonlinear dependencies. Hence, I is a natural way to quantify the deviation from independence of two processes. Throughout the paper we use a fixed threshold value of $v_{\text{th}} = 0.7$, which lies well above the noisy fixed point amplitudes of v (for not too large noise
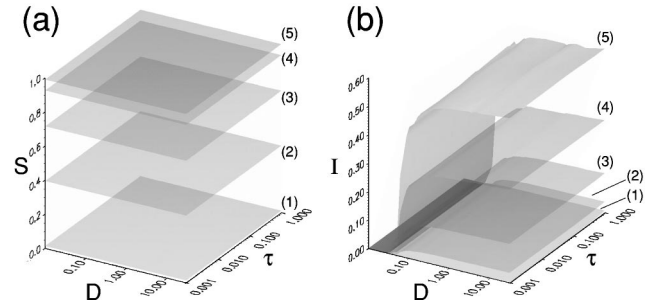
FIG. 1. The cross-correlation measure S (a) and the mutual information I (b) of the noise generated via Eq. (5) as a function of the noise strength D and temporal noise color τ. The square of the spatial correlation λ varies in (a) and (b) from (1) $\lambda^2 = 0.1$, (2) $\lambda^2 = 0.3$, (3) $\lambda^2 = 0.5$, (4) $\lambda^2 = 1.0$ to (5) $\lambda^2 = 5.0$. An integration time of $T = 700 \, t.u.$ with a sampling rate of $14 \, t.u.^{-1}$ was used. Four realizations of the noise have been performed, each time using a different set of random numbers. Other parameters values are given in Sec. II.

strengths and space color). Albeit changing v_{th} between 0.5 and 1.0 did not change the results for I significantly.

Before studying the noise-induced structures in Eq. (1), we apply these tools to a surrogate data test by using noise generated via Eq. (5). Figures 1(a) and 1(b) show the time averaged cross-correlation measure S and the mutual information I for various spatial correlations λ as a function of the noise strength D and the temporal noise color τ. Being measures for spatial coherence, both S and I increase with λ without showing any dependence on τ, as it should be. The normalization of S yields this quantity independent of the noise strength D. S saturates at $\lambda^2 \approx 2$, i.e., no further increase can be observed at higher spatial noise correlation. The state space discretization used for I on the other hand, induces another threshold for the noise strength ($D \approx 0.1$), below which I remains zero for all noise parameters, and above which I rises to a maximal value that is determined by λ. Consequently, the above analysis tools are capable of sorting out spatial correlations, irrespective of other noise parameters.

IV. RESULTS

The influence of the spatiotemporal noise on the structure formation in the network is depicted in the contour plots in Fig. 2. Figure 2(a) denotes the temporally almost white noise case ($\tau = 0.001$), while Fig. 2(b) is an example using some intermediate noise color ($\tau = 0.05$). First, note the optimal noise strength in Figs. 2(a) and 2(b) at which one perceives the most coherent spatial structures, like fragmented spirals and target waves [e.g., in 2(a) for $D = 10.0$ and $\lambda^2 = 0.1$]. The sole impact of increased τ is a shift of the optimal noise strength for pattern formation towards smaller values [compare the first two columns in Fig. 2a with the last two columns in Fig. 2(b)]. Changing the spatial noise correlation changes the appearance of the spatial structures themselves. Increasing λ reduces the small, irregular background fluctuations (left columns) and reshapes the spatial patterns to cloudy structures [bottom rows in Figs. 2(a) and 2(b)].
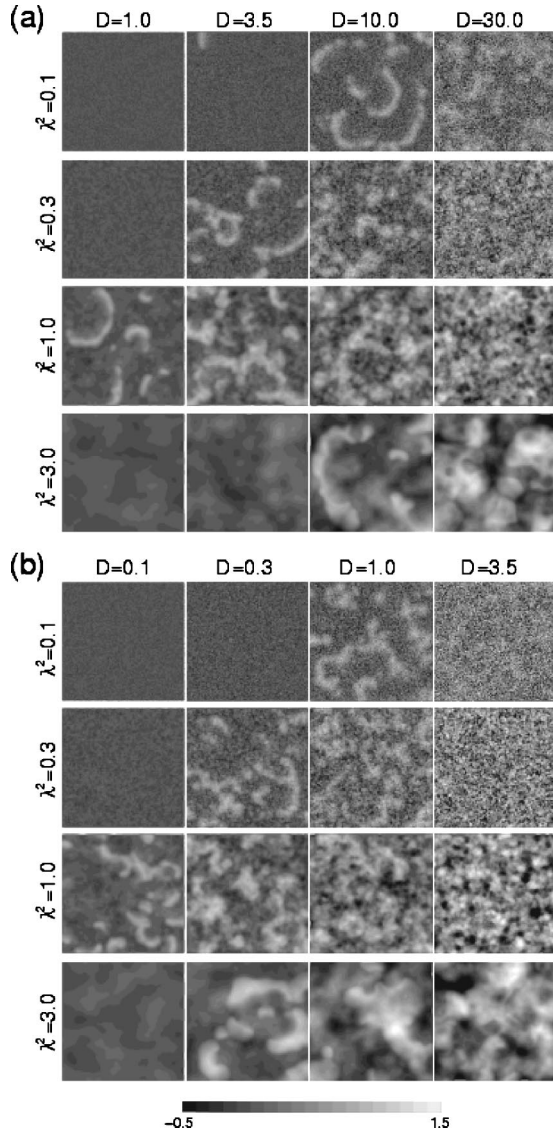
FIG. 2. Snapshots of the network for various noise strengths D (columns) and spatial noise color (rows) for 2 values of temporal correlations. (a) $\tau=0.001$ (b) $\tau=0.05$. Shown are the v variables of each grid point [Eq. (1)]. The amplitudes are color coded in 20 steps from -0.5 to 2.0. All snapshots have been taken after a transient of $50\,t.u.$ Other parameters values are given in Sec. II.

FIG. 3. The mutual information I (left column) and the cross-correlation measure S (right column) as a function of the noise strength D for various values of spatiotemporal noise color. τ increases from top to bottom, (a) and (f) $\tau=0.001$, (b) and (g) $\tau=0.01$, (c) and (h) $\tau=0.1$, (d) and (i) $\tau=1.0$ to (e) and (j) $\tau=10.0$. The spatial correlation in each plot increases from (1) $\lambda^2=0.001$ (bottom) via (2) $\lambda^2=0.05$, (3) $\lambda^2=0.3$, (4) $\lambda^2=0.4$, (5) $\lambda^2=0.5$, (6) $\lambda^2=1.0$ to (7) $\lambda^2=3.0$ (top). S and I have been calculated taking 2000 time series samples at a sampling rate of $0.31\,t.u.$ Error bars denote the variance of the data points obtained in quadruple. Varying v_{th} for calculation I did not change the results, qualitatively. For other parameter values cf. Sec. II.

The visual impression can be quantified by the cross-correlation measure S and the mutual information I. Figure 3 shows I and S as a function of spatiotemporal noise correlation in the left (a)–(e) and right (f)–(j) column, respectively. The temporal correlation of the noise increases from the top to the bottom row. A resonance-type behavior in D, indicating the signature of STSR, is detected by both I and S at all values of τ. Moreover, the noise strength at which the optimal noise-induced pattern formation is detected (D_{opt}), is changed by both the temporal and spatial noise color (Fig. 4).

Interestingly, S takes up the same values for small and large noise strengths D. This is a sign of the network dynamics in both cases being dominated by the stochastic forcing. Obviously, the network permanently shows stochastic oscil-

lations at high noise strength. If the variance of the noise is small, the individual network oscillators are incapable of performing oscillations. Hence, each element undergoes fluctuations around its stable fixed point, only. Because of S being a measure for the spatial coherence in the system, it thus renders the spatial correlation length λ of the underlying noise field in both cases. The maximum of S at intermediate noise strengths then indicates an increase of spatial correlations in
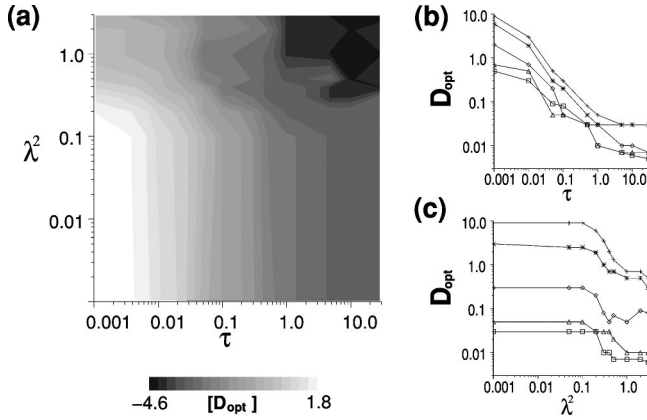
FIG. 4. (a) Contour plot of locations of the maxima (D_{opt}) obtained from the cross-correlation measure S [Eq. (13)] as a function of τ and λ^2. The contour levels increase logarithmically from $D = 0.01$ (black) to $D = 10.0$ (white). (b) Cross sections of the contour plot in (a) for constant values of the spatial correlation. λ increases from top to bottom with $\lambda^2 = 0.001$ (crosses), $\lambda^2 = 0.3$ (asterisk), $\lambda^2 = 0.4$ (diamonds), $\lambda^2 = 1.0$ (triangles), and $\lambda^2 = 3.0$ (squares). (c) Cross sections of the contour plot in (a) for constant values of the temporal correlation. τ increases from top to bottom with $\tau = 0.001$ (crosses), $\tau = 0.01$ (asterisk), $\tau = 0.1$ (diamonds), $\tau = 1.0$ (triangles), and $\tau = 10.0$ (squares). For parameters cf. Fig. 3.

the network due to an interplay of the stochastic forcing and the excitable dynamics, i.e., the occurrence of excitable pattern formation.

The influence of increasing temporal noise correlation τ is a shift of D_{opt} towards smaller noise strength. This change can be understood from the impact of the noise on the individual network oscillator. Close to their respective fixed point, the inhibitor variable v of each individual oscillator from Eq. (1) is dissipative with a slow exponential decay (the decay constant is of the order ≈ 1). Hence, the network elements act as a (temporal) low-pass frequency filter [27]. On the other hand, increasing τ, while keeping D, i.e., the total noise energy, constant, biases the energy distribution of the noise towards smaller temporal frequencies [cf. Eq. (10)]. Consequently, the fluctuations have an ever greater impact at low noise strengths D, causing the above described shift of D_{opt}.

Within a range of $0.01 \leq \tau \leq 1.0$, Fig. 4(b) shows that the position of D_{opt} as a function of the temporal correlation follows a power law, i.e., $D_{opt}(\tau) \propto \tau^{-\alpha}$. The characteristic exponent $\alpha \approx 1 \pm 0.05$ is almost independent of the spatial correlation. Consequently, $\sigma_{opt}^2 = \tau D_{opt}$, the optimal STSR noise *intensity*, remains constant within this range of τ. This indicates that the oscillators perceive the colored noise as white, due to their characteristic time scales being much larger than the temporal correlation of the noise. The power-law scaling becomes corrupted at large values of τ. Then, most energy of the noise is accumulated within the oscillators' limit cycle frequency ranges and a further increase of τ will not shift D_{opt} towards smaller values of the noise strength, as observed in Figs. 3(f)–3(j).

Also note how the variation of τ changes the STSR behavior of the network qualitatively. Due to the smoothing effect of using smaller noise strengths for inducing patterns in the system, the error bars at the onset of the resonant peak of S are diminished with increasing temporal noise correlation.

The variation of the spatial correlation λ results in two effects. Similar to the temporal noise color, increasing λ moves the position of D_{opt} towards smaller values of D, regardless of the value of τ [Fig. 4(c)]. This behavior can be explained on the network level. Excitations initiated at some point are more likely to spread, if there is an accumulation of favorable noise perturbations within their immediate neighborhood [5]. Spatial noise color will increase the susceptibility of local sites to excitation, as it renders them in a state similar to the site, where the wave was initiated. Thus, local excitations are more likely to spread with increasing spatial noise correlation length, but in contrast to the findings for varying temporal noise correlation, there is no power-law dependence of D_{opt} as a function of λ.

Furthermore, an increasing spatial correlation of the noise has a decremental effect on the overall occurrence of STSR. This finding can be related to the interplay of the spatial scales present in the noise and in the deterministic network. To achieve a certain degree of comparability, we fit a Gauss function to the front of a plane wave initiated through appropriate driving in the deterministic system. Using $v(\mathbf{r}) \propto \exp -(\mathbf{r}^2 \lambda_d^{-2})$ as a simple fit for the inhibitor variable, one finds $\lambda_d \approx 1$.

Depending on $r = \lambda/\lambda_d$, two different types of network behavior can be distinguished. For $0 \leq r \leq 1$ and $r \Rightarrow 1$, the absolute and relative maxima for S and I, respectively, become wider, moving towards smaller values of D as explained above. Local amplitude differences are decreased by the "ordering" effect of the spatial noise color, resulting in an increase of S with λ [Figs. 3(e)–3(h)]. At $r = 1$, pattern formation occurs over a wide range of noise strengths, as noise and intrinsic network correlations support each other in an optimal way. For $r > 1$ the shape of the spatial patterns changes from the typical excitation shapes to cloudlike structures [Figs. 2(a) and 2(b), bottom rows]. This transition is detected by the mutual information, only. S remains virtually unchanged for every value of D or τ, as a consequence of the high degree of synchronization of nearest neighbors. The delay in the rise of I with the noise strength D for $\lambda^2 = 3$ [Fig. 3(a)–3(c)] resembles the functional dependence of the mutual information on D in the pure noise case (Fig. 1), now indicating that noise is dominating the dynamics of the system. The change of the dynamical behavior in the network is also accompanied by large error bars for I. As now patterns render the spatial structure of the noise field rather than the underlying excitable network dynamics, the excitation threshold of the individual oscillators become more or less meaningless and one cannot distinguish between excited and quiescent states of the v_{ij}'s as clearly as before.

We want to stress, that the above discussion is valid for short temporal noise correlations, only. An increase in the temporal correlation of the noise has a non-negligible effect on the average excitability threshold of the individual oscillators in the network, which directly influences the oscillators' pulse shapes. Thus, at large τ, i.e., $\tau > 1.0 \, t.u.$, one can-

not assume the same λ_d for both the deterministic and the stochastic case. From Figs. 3(a)–3(e), one observes how the decremental effect of spatial noise correlation on STSR is counteracted by an increase in the temporal noise color. Local maxima in I, indicating the signature of STSR, which are not present for $\lambda^2 = 3$ in Figs. 3(a)–3(c), are restored for large values of τ [Fig. 3(e)].

V. DISCUSSION

In conclusion, we investigated the influence of spatiotemporal noise color and noise strength on structure formation in a network of coupled excitable systems using nearest-neighbor analysis tools. To our knowledge, this is the first time that STSR has been shown to occur in the Barkley system using additive spatiotemporal noise. Both spatial and temporal correlations have a favorable impact on STSR by causing a shift of D_{opt} towards smaller values of noise strengths. This has been explained as occurring due to an interplay of the noise's and the system's spatiotemporal length scales.

The phenomenon of noise-induced pattern formation is robust with respect to a wide range of temporal noise correlation parameters τ, but it disappears, if the spatial correlation of the noise exceeds that of the underlying excitable system, i.e., $\lambda > \lambda_d$. In this situation, the behavior of S and I with varying D equal the pure noise case, hinting that the dynamics of the network become noise dominated. A resonancelike behavior with respect to λ is observed, if the spatial length scales of the noise and the underlying deterministic system interfere. Then, the formation of coherent patterns occurs over a wide range of noise strengths, starting at small values of D, already.

Several open questions remain. Interestingly, we did not find a change in the network dynamics with increasing τ, as we did for an increasing spatial noise correlation. Quite contrary, in the parameter regimes investigated, the temporal noise correlation seems to have a stabilizing effect on the excitable dynamics of the network and thus on STSR. Hence, further investigations should extend to investigating space-time neighborhoods for S and I, thus gaining information on the interdependence of the spatial and temporal length scales of the noise and the underlying deterministic network. Moreover, it would be worthwhile to develop an analytical framework for the dependence of STSR on additive spatiotemporal colored noise, as recently has been put forward by Alonso *et al.* [28] for the case of multiplicative noise. There, the authors have shown that one is able to replace spatially extended media, driven by spatiotemporally colored multiplicative noise, with an effective deterministic reaction-diffusion equation, their analytical results being in very good agreement with numerical simulations, as well as experimental data, for both the excitable and oscillatory regimes.

Investigating the influence of noise correlation parameters on pattern formation may provide further insight into the interpretation of data from biological time series and modeling. The combined influence of external and internal noise (e.g., fluctuating environment conditions versus intrinsic thermal fluctuations) can result in new dynamical behavior of the underlying deterministic system. In a recent experimental study it was observed that the dynamics of the photosynthetic efficiency in a circadian rhythm of a plant leaf show spatiotemporal separation of the photosynthetic metabolism activity [29]. Previous models of plant leaf dynamics with spatially extended excitable media could not predict these patchy structures observed in experiment. It is possible that the inclusion of spatiotemporally correlated (stochastic) forces, e.g., entering the experiment through the spatial variation of the light intensity, could render the model simulations closer to the experimental data [30].

[1] M. Cross, and P. Hohenberg, Rev. Mod. Phys. **65**, 851 (1993).

[2] D. Wallgraef, *Spatio-Temporal Pattern Formation* (Springer, New York, 1996).

[3] P. Jung and G. Mayer-Kress, Chaos **5**, 458 (1995); P. Jung and G. Mayer-Kress, Phys. Rev. Lett. **74**, 2134 (1995).

[4] H. Hempel, L. Schimansky-Geier, and J. García-Ojalvo, Phys. Rev. Lett. **82**, 3713 (1999).

[5] J. Wang, S. Kádár, P. Jung, and K. Showalter, Phys. Rev. Lett. **82**, 855 (1999).

[6] S. Alonso, I. Sendiña-Nadal, V. Pérez-Munuzuri, J.M. Sancho, and F. Sagués, Phys. Rev. Lett. **87**, 078302 (2001).

[7] J. García-Ojalvo and L. Schimansky-Geier, Europhys. Lett. **47**, 298 (1999).

[8] V. Pérez-Muñuzuri, F. Sagués, and J.M. Sancho, Phys. Rev. E **62**, 94 (2000).

[9] Y. Zhou, and P. Jung, Europhys. Lett. **49**, 695 (2000).

[10] S. Kádár, J. Wang, and K. Showalter, Nature (London) **391**, 770 (1998).

[11] P. Jung, A.H. Cornell-Bell, K. Madden, and F. Moss, J. Neurophysiol. **70**, 1098 (1998).

[12] H. Busch, M.-Th. Hütt, and F. Kaiser, Phys. Rev. E **64**, 021105 (2001).

[13] C. Hauptmann, F. Kaiser, and C. Eichwald, Int. J. Bifurcation Chaos Appl. Sci. Eng. **9**, 1159 (1999).

[14] M. Elowitz, A. Levine, W. Siggla, and P. Swain, Science **297**, 1183 (2002).

[15] I. Sendiña-Nadal and Pérez-Munuzuri, Int. J. Bifurcation Chaos Appl. Sci. Eng. **11**, 2837 (2001).

[16] P. Jung, J. Wang, R. Wackerbauer, and K. Showalter, Phys. Rev. E **61**, 2095 (2000).

[17] I. Goychuk and P. Hänggi, Phys. Rev. E **61**, 4272 (2000).

[18] C.E. Shannon and W. Weaver, *The Mathematical Theory of Information* (University of Illinois Press, Urbana, IL, 1949).

[19] M.-Th. Hütt, R. Neff, H. Busch, and F. Kaiser, Phys. Rev. E **66**, 026117 (2002).

[20] D. Barkley, M. Kness, and L.S. Tuckermann, Phys. Rev. A **42**, 2489 (1990).

[21] M. Dowle, R. Mantel, and D. Barkley, Int. J. Bifurcation Chaos Appl. Sci. Eng. **7**, 2529 (1997).

[22] M. Bär and M. Eiswirth, Phys. Rev. E **48**, R1635 (1993).

[23] H. Zhonghuai, Y. Lingfa, X. Zuo, and X. Houwen, Phys. Rev. Lett. **81**, 2854 (1998).

[24] H. Ito and L. Glass, Phys. Rev. Lett. **66**, 671 (1991).

[25] M. Bär, N. Gottschalk, M. Eiswirth, and G. Ertl, J. Chem. Phys. **100**, 1202 (1994).

[26] J. Garcfia-Ojalvo and J.M. Sancho, *Noise in Spatially Extended Systems* (Springer, New York, 1999).

[27] D. Nozaki, J.J. Collins, and Y. Yamamoto, Phys. Rev. E **60**, 4637 (1999).

[28] S. Alonso, F. Sagués, and J.M. Sancho, Phys. Rev. E **65**, 066107 (2002).

[29] U. Rascher, M.-Th. Hütt, K. Siebke, B. Osmond, F. Beck, and U. Lüttge, Proc. Natl. Acad. Sci. U.S.A. **98**, 11801 (2001).

[30] A. Bohn and F. Kaiser (private communication).